Korean J Physiol Pharmacol 2018;22(1):23-33
https://doi.org/10.4196/kjpp.2018.22.1.23

KJPP

Original Article

Histone deacetylase inhibition attenuates hepatic steatosis in rats with experimental Cushing's syndrome

Mina Kim[1,2,3,4], Hae-Ahm Lee[1,2,3], Hyun-Min Cho[1], Seol-Hee Kang[1,2,3,4], Eunjo Lee[1,2,3,4], and In Kyeom Kim[1,2,3,4,*]

[1]Department of Pharmacology, [2]Cardiovascular Research Institute, [3]Cell and Matrix Research Institute, [4]BK21 Plus KNU Biomedical Convergence Program, Department of Biomedical Science, Kyungpook National University School of Medicine, Daegu 41944, Korea

ARTICLE INFO

Received March 29, 2017
Revised July 14, 2017
Accepted July 30, 2017

***Correspondence**
In Kyeom Kim
E-mail: inkim@knu.ac.kr

Key Words
Cushing's syndrome
Glucocorticoid receptor
HDAC inhibitor
Hepatic steatosis
Sodium valproate

ABSTRACT Cushing's syndrome (CS) is a collection of symptoms caused by prolonged exposure to excess cortisol. Chronically elevated glucocorticoid (GC) levels contribute to hepatic steatosis. We hypothesized that histone deacetylase inhibitors (HDACi) could attenuate hepatic steatosis through glucocorticoid receptor (GR) acetylation in experimental CS. To induce CS, we administered adrenocorticotropic hormone (ACTH; 40 ng/kg/day) to Sprague-Dawley rats by subcutaneous infusion with osmotic mini-pumps. We administered the HDACi, sodium valproate (VPA; 0.71% w/v), in the drinking water. Treatment with the HDACi decreased steatosis and the expression of lipogenic genes in the livers of CS rats. The enrichment of GR at the promoters of the lipogenic genes, such as acetyl-CoA carboxylase (*Acc*), fatty acid synthase (*Fasn*), and sterol regulatory element binding protein 1c (*Srebp1c*), was markedly decreased by VPA. Pan-HDACi and an HDAC class I-specific inhibitor, but not an HDAC class II a-specific inhibitor, attenuated dexamethasone (DEX)-induced lipogenesis in HepG2 cells. The transcriptional activity of *Fasn* was decreased by pretreatment with VPA. In addition, pretreatment with VPA decreased DEX-induced binding of GR to the glucocorticoid response element (GRE). Treatment with VPA increased the acetylation of GR in ACTH-infused rats and DEX-induced HepG2 cells. Taken together, these results indicate that HDAC inhibition attenuates hepatic steatosis through GR acetylation in experimental CS.

INTRODUCTION

Cushing's syndrome (CS) is caused by prolonged elevation of the levels of circulating cortisol [1]. The levels of circulating cortisol, a principal glucocorticoid (GC), are controlled by the hypothalamic-pituitary-adrenal axis [2]. The anterior pituitary gland secretes adrenocorticotropic hormone (ACTH), which stimulates secretion of cortisol by the adrenal glands [3]. CS is characterized by central obesity, insulin resistance, hypercholesterolemia, diabetes, and muscle wasting [4]. The chronically elevated GC levels that occur in CS also cause hepatic steatosis [5].

GCs are steroid hormones that play critical and complex roles in the maintenance of metabolic homeostasis and lipid metabolism [6,7]. The effects of GCs are mediated via the glucocorticoid receptor (GR), a member of the nuclear receptor superfamily of transcription factors. Upon binding to GC in the cytosol, the GR translocates into the nucleus where it functions as a transcriptional regulator of GC-responsive target genes via direct DNA binding or through protein-protein interactions with other transcriptional coregulators [8]. GCs are potent, key regulators that drive lipogenesis through the upregulation of fatty acid synthase (*Fasn*), acetyl-CoA carboxylase (*Acc*), stearoyl-CoA desaturase-1 (*Scd1*) [9], and sterol regulatory element binding protein 1c (*Srebp1c*) [10,11]. However, the molecular mechanism by which the GR induces hepatic lipogenesis and steatosis is largely unknown.

Posttranslational modifications of steroid receptors, such as

Author contributions: M.K. wrote the manuscript, performed the cell-based experiments (except Fig. 3. and Fig. 7B), performed animal based experiments (except Fig. 9B, C) and bred animals. H.A.L. organized the study, performed immunoprecipitation in Fig. 9C. H.M.C. performed Chip assay in Fig. 3. and EMSA in Fig. 7B. S.H.K. and E.L. helped breed and I.K.K. supervised the study.

phosphorylation, acetylation, ubiquitylation, and sumoylation, are important mechanisms for the regulation of target gene expression [12]. The phosphorylation of GR is critical to its ability to regulate the expression of target genes involved in insulin signaling and lipid metabolism, thereby potentially facilitating insulin resistance [13]. The acetylation of GR also controls the activity of various cytosolic and nuclear proteins [14].

HDAC inhibitors including valproic acid (VPA) have been reported to exert several beneficial effects in T2DM and its complications [15,16]. VPA is primarily used for the treatment of epilepsy, migraine and bipolar disorders. VPA has been proven as an HDAC inhibitor and subdued the activities of class I and II HDACs. HDAC inhibitors (HDACi) increase transcription via chromatin decondensation [17]. However, recent studies have reported that HDACi can also suppress the expression of genes [18,19]. Our previous study revealed that acetylation of the mineralocorticoid receptor caused by HDAC inhibition attenuates its transcriptional activity and the expression of target genes [20,21]. Few studies have investigated whether HDACi prevent steatosis and lipogenesis in the context of excess GCs, as associated with CS. We hypothesized that HDACi could attenuate hepatic steatosis through GR acetylation in experimental CS.

METHODS

Animals

The study was conducted in accordance with the National Institutes of Health Guide for the Care and Use of Laboratory Animals, after approval by the Institutional Review Board of Kyungpook National University; every effort was made to minimize both the number of animals used and their suffering. Nine-week-old male Sprague-Dawley (SD) rats were unilaterally nephrectomized under ketamine (150 mg/kg; Yuhan, Seoul, Korea) and xylazine (18 mg/kg; Bayer, Seoul, Korea) anesthesia, as previously described [21]. Rats received subcutaneous infusion of ACTH (40 ng/kg/day) via an osmotic mini-pump. Sodium valproate (VPA) was purchased from Sigma-Aldrich (St. Louis, MO, USA). VPA (0.71% w/v) was administered via the drinking water for 4 weeks. Rats were anesthetized with sodium pentobarbital (50 mg/kg intraperitoneally). Tissues were frozen in liquid nitrogen and stored at –80°C until further study.

Cell culture

HepG2 cells were purchased from the American Type Culture Collection (Manassas, VA, USA) and maintained under 5% CO_2 at 37°C in Dulbecco's modified Eagle's medium with L-glutamine and 4,500 mg/L glucose containing 10% fetal bovine serum (Invitrogen, Carlsbad, CA, USA). They were sub-cultured every 3 or 4 days with trypsin (0.25%) and EDTA (0.02%). A fraction of the detached cells was transferred to normal Tyrode's solution and kept at 4°C in microtubes. We treated HepG2 cells with the HDACi; VPA (Sigma-Aldrich Inc., MO, USA), SAHA (Sigma-Aldrich Inc., MO, USA), TSA (Sigma-Aldrich Inc., MO, USA), MS275 (Selleckchem, TX, USA) and MC1568 (Santa Cruz Biotechnology, CA, USA), then incubated the cells with or without DEX.

Histology

For trichrome, Oil Red O, and hematoxylin&eosin (H&E) stains, liver tissues were fixed in 4% formalin overnight, then dehydrated and embedded in paraffin. The paraffin-embedded samples were sectioned at a thickness of 3 mm. The slides were examined using light microscopy.

Oil Red O stain

Briefly, to examine the accumulation of fat, HepG2 cells were rinsed with cold phosphate-buffered saline (PBS) and fixed in 10% paraformaldehyde for 30 min. After the cells were washed with 60% isopropanol, they were stained for at least 1 h in a freshly diluted Oil Red O solution (6 parts 0.5% Oil Red O in isopropanol stock solution and 4 parts H_2O). After the stain was removed and the cells were washed with 60% isopropanol, images of each group of cells were acquired (Nikon Imaging Korea, Seoul, Korea).

Quantitative reverse transcription-polymerase chain reaction (RT-qPCR)

RT-qPCR was performed using an ABI PRISM® 7000 Sequence Detection System (Applied Biosystems, Foster City, CA, USA) as previously described [21]. Amplification reactions containing 10 μL of SYBR® Green PCR Master Mix (Applied Biosystems), 4 μL of cDNA, and the indicated primer set (200 nM) were performed in a total volume of 20 μL. All samples were amplified in triplicate in a 96-well plate, with the following cycling conditions: 2 min at 50°C, 10 min at 95°C, and 40 cycles at 95°C for 15 s followed by 1 min at 60°C. The relative mRNA expression level was determined by calculating the values of Δcycle threshold (ΔCt) by normalizing the average Ct value compared to its endogenous control (*Gapdh*), then calculating $2^{-\Delta\Delta Ct}$. Statistical analyses were performed using one-way analysis of variance (ANOVA). The primer sets are given in the supplementary data (Table 1S).

Immunoprecipitation and Western blotting

The frozen tissues were homogenized in RIPA buffer containing protease inhibitors. The cell lysates were precleared with protein G agarose at 4°C for 2 h. The supernatants were incubated overnight with 1 mg of GR antibody (Santa Cruz Biotechnology, USA), or acetyl-lysine (ac-K) antibody (Cell Signaling Technology,

USA), at 4°C. The immunocomplexes were washed 3 times with lysis buffer (20 mM Tris, 150 mM NaCl, 1% NP-40, 0.5% SDS, 0.1% SDS, and 1 proteinase inhibitor cocktail), then subjected to western blot analysis. For western blots, protein-matched samples (Bradford assay) were subjected to SDS-PAGE, then transferred to nitrocellulose membranes. The nitrocellulose membranes were blocked with 5% skim milk in TBS (25 mM Tris base and 150 mM NaCl) for 2 h at room temperature, then incubated with 1 mg/mL of GR or ac-K antibody at 4°C overnight. Then, the membranes were incubated in secondary antibody (diluted 1:5000) at room temperature for 1 h, and washed 3 times for 10 min each in TBST. The target proteins were detected with Enhanced Chemiluminescence Plus detection reagents (Amersham, Pittsburgh, PA, USA). The expression levels were quantified by optical densitometry (ImageJ software; http://rsbweb.nih.gov). We performed western blotting with the following antibodies: GR antibody (Santa Cruz Biotechnology, CA, USA), SREBP1 antibody (Santa Cruz Biotechnology, CA, USA), ac-K antibody (Cell Signaling Technology, MA, USA), ACC antibody (Thermo Fisher, MA, USA) FAS antibody (Thermo Fisher, MA, USA), GAPDH antibody (Thermo Fisher, MA, USA), SCD1 antibody (Abcam, Cambridge, UK), and β-actin antibody (Sigma-Aldrich Inc., MO, USA).

Electrophoretic mobility shift assay (EMSA)

Oligonucleotides were either commercially synthesized or, in the case of the oligonucleotide glucocorticoid response element (GRE), obtained from Genotech (Pohang, Korea). The oligonucleotides that we used in the EMSAs included 35 nucleotides of GCs. Complementary oligonucleotides in equimolar amounts were heated to 100°C, cooled overnight to 25°C, divided into aliquots, and stored at –20°C before use. Double-stranded oligonucleotide probes were end-labeled using T4 polynucleotide kinase and [γ-^{32}P]-ATP. Binding reactions were performed in a 20-mL volume containing approximately 20,000 cpm of labeled probe, 6~12 mg of nuclear extract, 20 mM HEPES (pH 7.9), 60 mM KCl, 5 mM $MgCl_2$, 2 mM dithiothreitol, 10% glycerol, 200 ng poly(dIzdC), 1 mg bovine serum albumin, and unlabeled competitor oligonucleotides. We followed the instructions provided by the manufacturer for EMSAs with the human recombinant GR. The binding reaction mixtures were incubated at 25°C for 30 min, then loaded onto 6% non-denaturing polyacrylamide gels in 25 mM Tris (pH 8.3), 25 mM boric acid, and 0.5 mM EDTA. For supershift experiments, incubations with polyclonal anti-human GR antibody from Abcam (Cambridge, UK) or preimmune antiserum (diluted 1:500) were performed for 30 min at room temperature after addition of radiolabeled GRE 5 and nuclear extract. Gels were dried and autoradiographed overnight at 270°C, using Fujifilm RX-Fuji medical X-ray film and intensifying screens. Epstein-Barr Nuclear Antigen (EBNA) extract was used as a positive control.

Chromatin immunoprecipitation (ChIP) assay

ChIP assays were performed according to the manufacturer's instructions, with minor modifications, using the EZ-ChIP™ kit (Upstate Biotechnology, Lake Placid, NY, USA) as previously described [22]. In brief, tissues were fixed with 1% formaldehyde and washed with ice-cold PBS. After homogenization, tissues were incubated in SDS lysis solution for 10 min on ice. The lysates were sonicated with 15 cycles of 100 amplitude for 10 s followed by cooling on ice for 50 s. The lysates were precleared with protein G agarose beads for 2 h. Then, antibodies were added and incubated at 4°C overnight. The antibody against GR was obtained from Abcam. Anti–polymerase II antibodies were obtained from Upstate Biotechnology. To reverse the crosslinking between DNA and chromatin, elutes were incubated at 65°C for 5 h after the addition of NaCl to a final concentration of 0.2 M. The proteins were eliminated by digestion with proteinase K at 45°C for 2 h and the DNA was purified with a spin column. Specific promoter DNA was quantified by qPCR. All samples were amplified in triplicate in 96-well plates, with the following cycling conditions: 2 min at 50°C, 10 min at 95°C, and 40 cycles at 95°C for 15 s followed by 1 min at 60°C. The primer sets are given in the supplementary data (Table 2S).

Luciferase assay

For the luciferase assay, HepG2 cells were seeded on collagen I-coated 12-well plates, cultured overnight, and transfected with vector constructs using Superfect Transfection Reagent (Qiagen, Hilden, Germany), according to the manufacturer's recommendation. The next day, cells were exposed to dexamethasone (DEX, 10 nmol/L) for 24 h with or without pretreatment with VPA (10 mmol/L). The cells were lysed with a lysis buffer and the luciferase activity was analyzed with a Bright-Glo™ Luciferase Assay System kit (Promega, Madison, WI, USA) according to the manufacturer's instructions. Luminescence was measured with a Veritas™ Microplate Luminometer (Turner Biosystems, Sunnyvale, CA, USA).

Statistics

Results are expressed as mean±standard error (SE). Data were analyzed with the Kruskal-Wallis test or one-way ANOVA followed by post hoc Tukey's comparison test; differences were considered significant at $p<0.05$. Student's t-test was applied for the analysis of the significance of differences between 2 groups. The procedures were performed using SPSS software (release 19.0, SPSS, Chicago, IL, USA).

RESULTS

VPA attenuated hepatic steatosis in ACTH-infused rats

To determine whether VPA has an anti-steatotic effect *in vivo*, we administered VPA into control SD rats or SD rats subcutaneously infused with ACTH for 4 weeks. Upon assessment of liver morphology and Oil Red O staining, we found that the administration of VPA considerably reduced ACTH-induced steatosis. We also examined collagen deposition and fibrosis, which would appear blue after trichrome staining. ACTH infusion did not affect liver collagen deposition and fibrosis (Fig. 1). We analyzed the expression of the lipogenic genes *Acc*, *Fasn*, *Scd1*, and *Srebp1c* by RT-qPCR. The ACTH-induced increase in the expression of *Acc*, *Fasn*, *Scd1*, and *Srebp1c* was attenuated by VPA (Figs. 2A~D). We confirmed the effect at the protein level by western blot analysis (Fig. 2E). Importantly, hepatic steatosis was reduced by VPA, which was associated with significantly reduced mRNA expression and protein levels of lipogenesis in the livers. These results suggested that HDAC inhibition may prevent hepatic steatosis in ACTH-infused rats by suppressing lipogenesis.

VPA reduced the ACTH-induced enrichment of GR and RNA polymerase II (Pol II) at target gene promoters in rats

We next analyzed the enrichment of GR and Pol II on the promoters for *Acc*, *Fasn*, *Scd1*, and *Srebp1c* by ChIP assay followed by qPCR (Fig. 3). The qPCR results showed that VPA attenuated the ACTH-induced enrichment of GR and Pol II at the *Acc*, *Fasn*, and *Srebp1c* promoters in rats compared with controls (Figs. 3A, 3B and 3D). VPA did not affect the enrichment of GR induced by ACTH at the *Scd1* promoter (Fig. 3C). These findings suggested that treatment with an HDACi decreased the recruitment of GR and Pol II to the promoters of lipogenesis-related genes *in vivo*.

DEX increased lipid accumulation in HepG2 cells

To further explore the molecular mechanism of the HDACi-induced reduction of liver steatosis, we developed an *in vitro* model of hepatic steatosis by exposing HepG2 cells to DEX (10 nmol/L). We investigated the expression of *Acc*, *Fasn*, *Scd1*, and *Srebp1c* using RT-qPCR. In HepG2 cells, Oil Red O stain indicated that DEX induced lipid accumulation in a dose-dependent manner (Fig. 4A). In addition, DEX increased the expression of lipogenesis genes in a dose- and time-dependent manner (Figs. 4B and C). Thus, DEX increased lipogenesis and lipid accumulation in HepG2 cells.

HDAC inhibition attenuated lipogenesis in HepG2 cells

We used VPA to determine whether HDAC inhibition could influence the DEX-mediated induction of lipogenesis. Pretreatment with VPA for 6 h attenuated DEX-induced expression of *Acc* (Fig. 5A), *Fasn* (Fig. 5B), *Scd1* (Fig. 5C), and *Srebp1c* (Fig. 5D). DEX increased expression of lipogenesis genes, which was attenu-

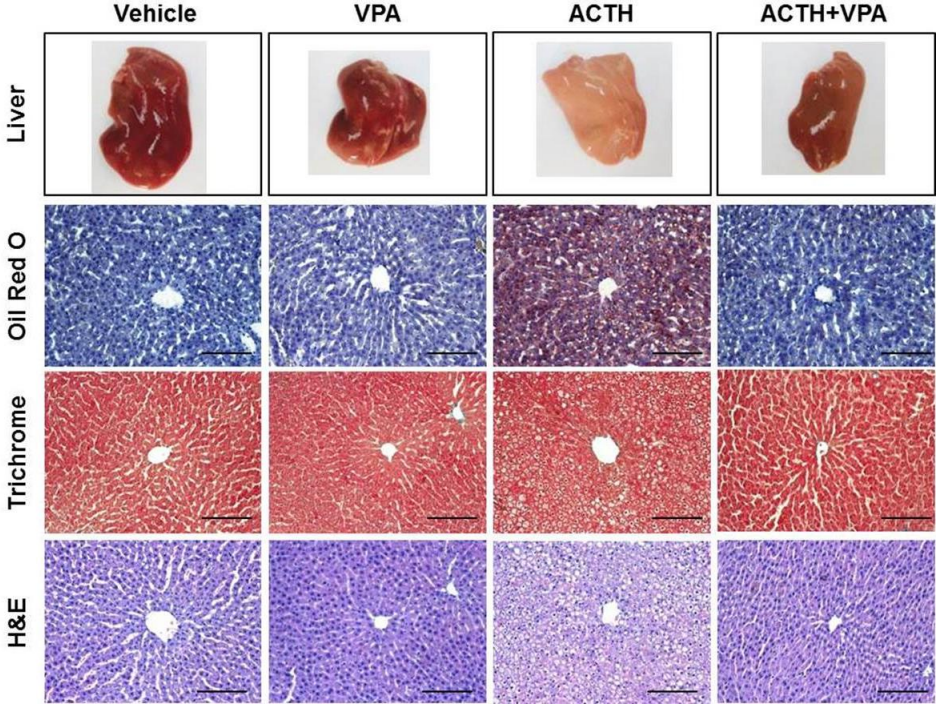

Fig. 1. Effects of VPA treatment on ACTH-induced steatosis. Representative images of livers from rats treated with vehicle (n=6), VPA (n=7), ACTH (n=6), or ACTH with VPA (n=7). Liver sections were stained with Oil Red O, trichrome, or H&E to compare between treatment groups. (Bar=50 μm, stain magnification 200×).

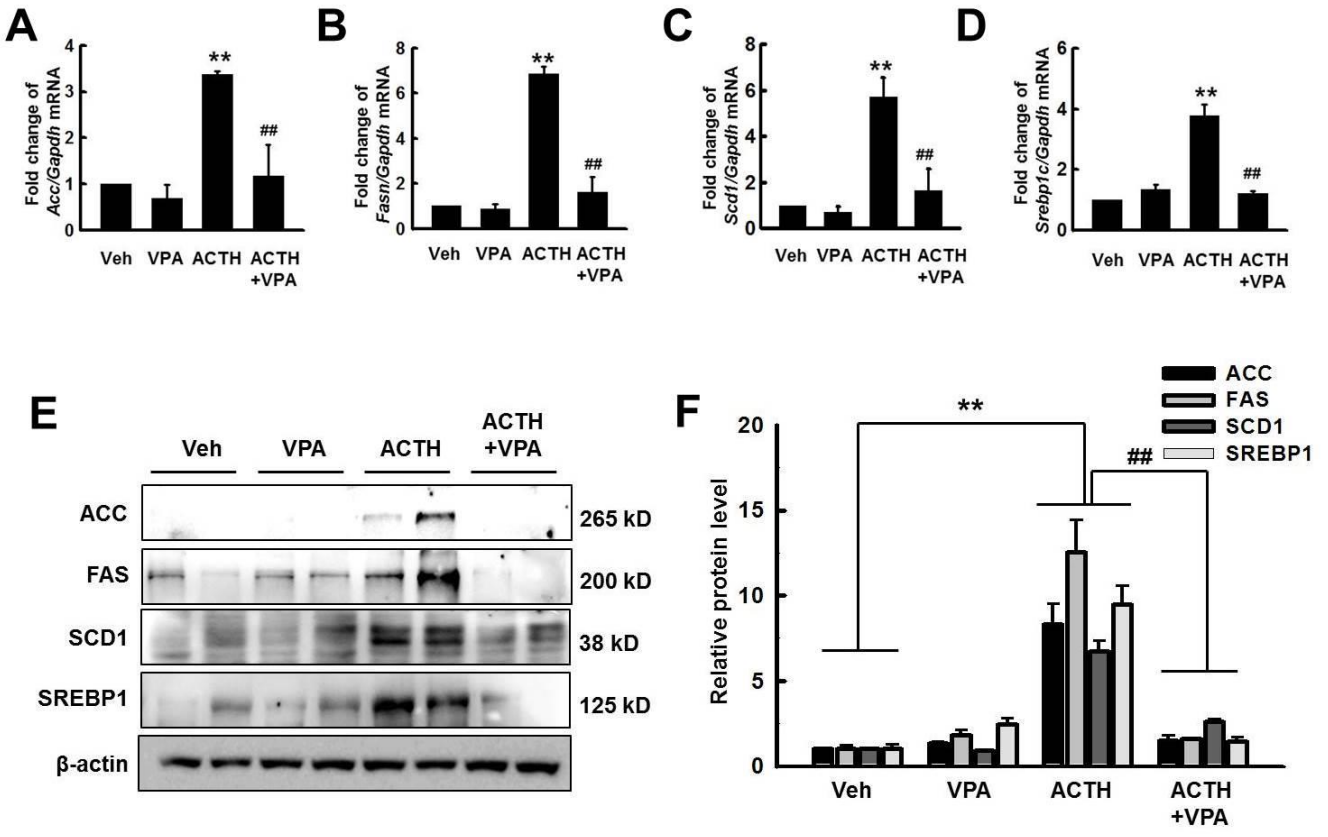

Fig. 2. Effects of VPA treatment on the expression of lipogenesis genes in the liver. Expression of lipogenesis genes *Fasn* (A), *Acc* (B), *Scd1* (C), and *Srepb1c* (D) was quantified by RT-qPCR. VPA treatment decreased the expression of lipogenesis genes in ACTH-induced rats. (E) The expression of lipogenesis proteins was detected by western blotting. (F) Relative protein expression was quantified by optical densitometry (ImageJ software; http://rsbweb.nih.gov). VPA treatment decreased lipogenesis protein expression in ACTH-induced rats. The graphs show the mean±SE of 3 independent experiments. *p<0.05 and **p<0.01 *vs.* control; #p<0.05 and ##p<0.01 *vs.* ACTH.

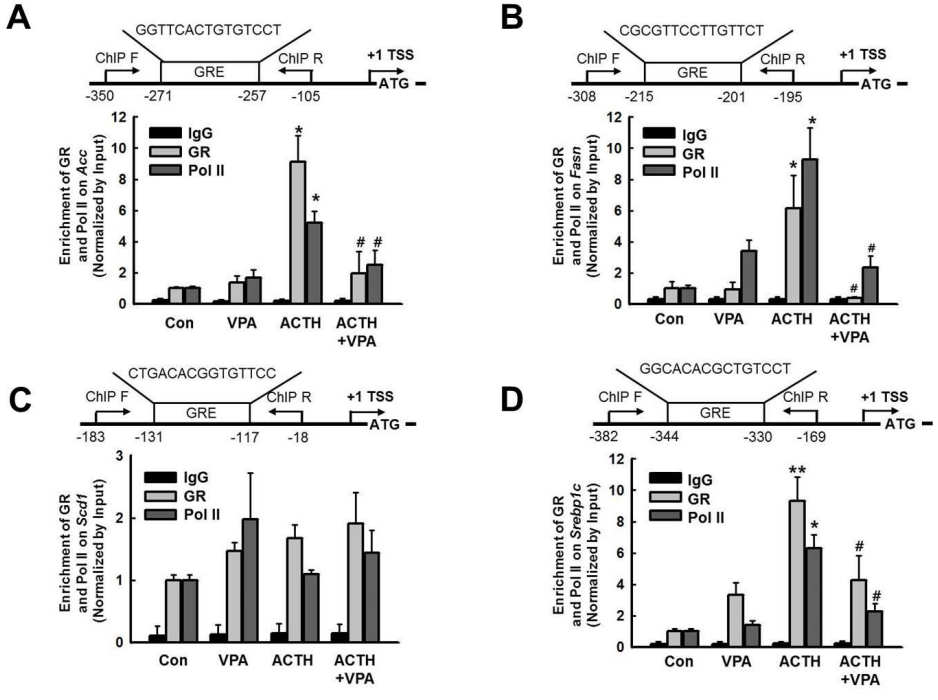

Fig. 3. Effect of VPA treatment on the enrichment of GR and RNA polymerase II (Pol II) onto the promoters of target genes in the rat liver. The enrichment of GR and Pol II at promoters of lipogenesis genes was analyzed by ChIP. Schematic diagrams show the locations of the GREs, as well as the PCR amplifications following the ChIP assay, for the *Fasn* (A), *Acc* (B), *Scd1* (C), and *Srebp1c* (D) promoters (upper). TSS; transcription start site. The ChIP assays were quantified by qPCR. ACTH infusion increased enrichment of GR and Pol II on *Fasn*, *Acc*, and *Srebp1c*, which were decreased by VPA treatment. The graphs show the mean±SE of 5 independent experiments. *p<0.05 and **p<0.01 *vs.* control; #p<0.05 and ##p<0.01 *vs.* ACTH.

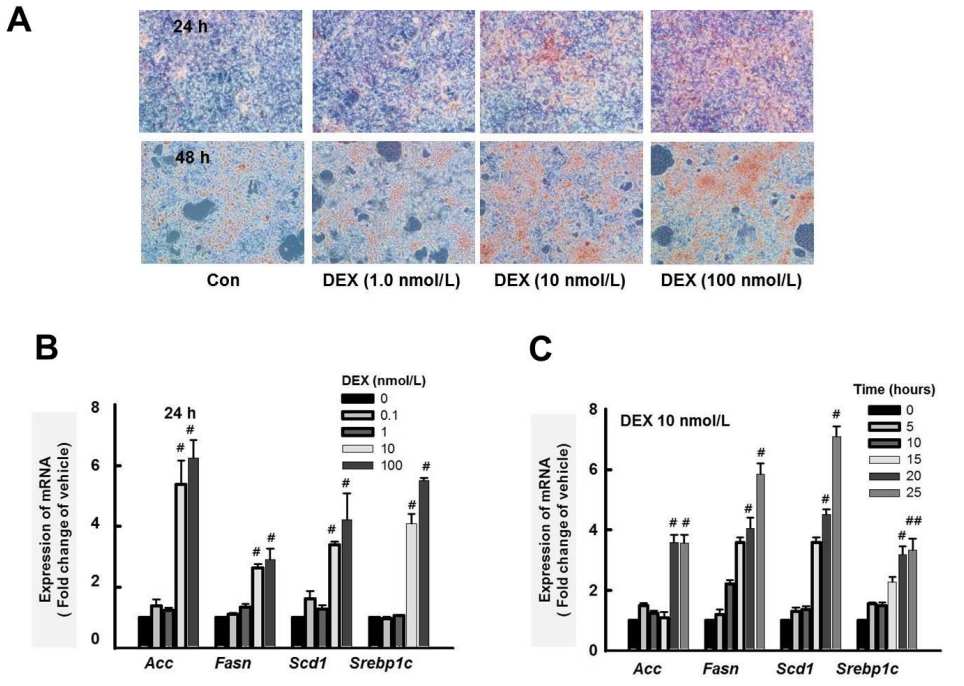

Fig. 4. Effect of dexamethasone (DEX) on lipid accumulation in HepG2 cells. (A) HepG2 cells were treated with DEX (1.0, 10, and 100 nM) for 24 and 48 h. Lipid accumulation was analyzed by Oil Red O staining. Original magnification, 40×. (B) *Acc*, *Fasn*, *Scd1*, and *Srepb1c* expression levels were quantified by RT-qPCR. Treatment with DEX for 24 h increased expression of *Acc*, *Fasn*, *Scd1*, and *Srepb1c* in a dose-dependent manner in HepG2 cells. (C) DEX (10 nM) increased the expression of *Acc*, *Fasn*, Scd1, and *Srepb1c* in a time-dependent manner. The graphs show the mean±SE of 3 independent experiments. $^{\#}p<0.05$, $^{\#\#}p<0.001$ *vs.* vehicle.

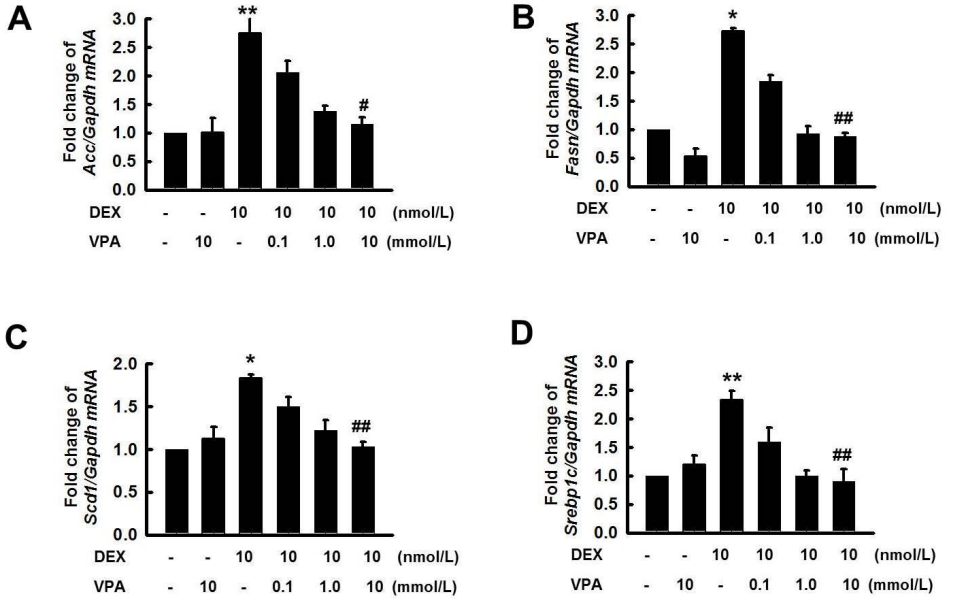

Fig. 5. Effect of VPA treatment on expression of lipogenesis genes by DEX in HepG2 cells. The expression of lipogenesis genes *Acc* (A), *Fasn* (B), *Scd1* (C), and *Srepb1c* (D) was quantified by RT-qPCR. HepG2 cells were pretreated with VPA (0.1, 1.0 and 10 mM) for 6 h then incubated with DEX (10 nM) for 24 h. Pretreatment with VPA decreased the DEX-induced expression of lipogenesis genes in a dose-dependent manner. The graphs show the mean±SE of 3 independent experiments *p<0.05, **p<0.01 *vs.* control; $^{\#}p<0.05$, $^{\#\#}p<0.01$ *vs.* DEX.

ated by VPA in HepG2 cells. Thus, we consider VPA a potential therapeutic agent for the treatment of lipogenesis. However, VPA is a pan-HDACi. To identify which type of HDACi affected DEX-induced lipid accumulation, we treated HepG2 cells with the pan-HDACi VPA, SAHA, and TSA; the HDAC class I-specific inhibitor MS275; and the HDAC class II a-specific inhibitor MC1568 for 6 h, then incubated the cells with or without DEX for 48 h. Pan-HDACi and the HDAC class I-specific inhibitor decreased DEX-induced lipid accumulation (Fig. 6A) and expression of *Srebp1c* (Fig. 6B) in HepG2 cells.

VPA reduced the recruitment and DNA binding affinity of GR

We analyzed the enrichment of GR and Pol II at the promoters of *Srebp1c* by ChIP assay followed by qPCR in HepG2 cells (Fig. 7A). The qPCR results revealed that the enrichment of GR and Pol II on the *Srebp1c* promoters induced by DEX, compared with the control, was attenuated by VPA. To examine the effect of VPA on DEX-induced GR DNA binding activity, we performed EMSAs. Treatment with DEX (10 nM) induced the formation of a strong binding complex (Fig. 7B, lane 4). Formation of the binding com-

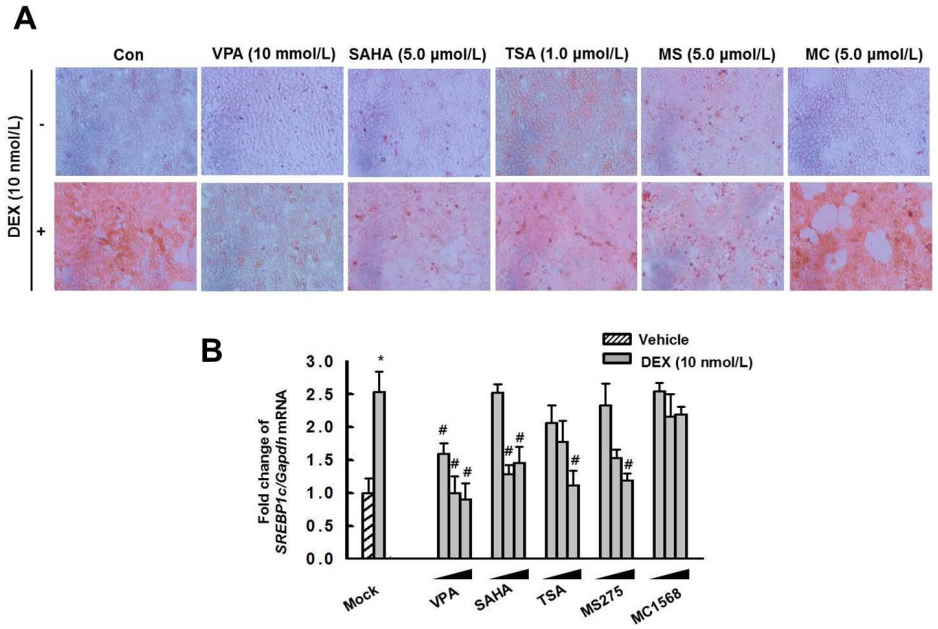

Fig. 6. Effect of HDAC inhibitors on lipid accumulation and expression of *Srepb1c* by DEX in HepG2 cells. HepG2 cells were pretreated with VPA (10 mM), SAHA (5.0 μM), TSA (1.0 μM), MS275 (5.0 μM), and MC1568 (5.0 μM) for 6 h then incubated with or without DEX (10 nM) for 48 h. Lipid accumulation was analyzed by Oil Red O stain. Original magnification, 40×. (B) Cells were pretreated with VPA (0.1, 1.0, and 10 mM), SAHA (0.1, 1.0, and 10 μM), TSA (0.1, 0.3, and 1.0 μM), MS275 (1.0, 10, and 100 μM), and MC1568 (0.1, 5.0, and 10 μM) for 6 h then incubated with DEX (10 nM) for 48 h. The expression of *Srebp1c* was quantified by RT-qPCR. Treatment with DEX increased lipid accumulation and the expression of *Srebp1c*, which were decreased by pretreatment with the pan-HDACi VPA, SAHA and TSA, or the HDAC class I-specific inhibitor MS275, but not with the HDAC class II a-specific inhibitor MC1568. The graphs show the mean±SE of 3 independent experiments. #p<0.05 *vs.* the mock.

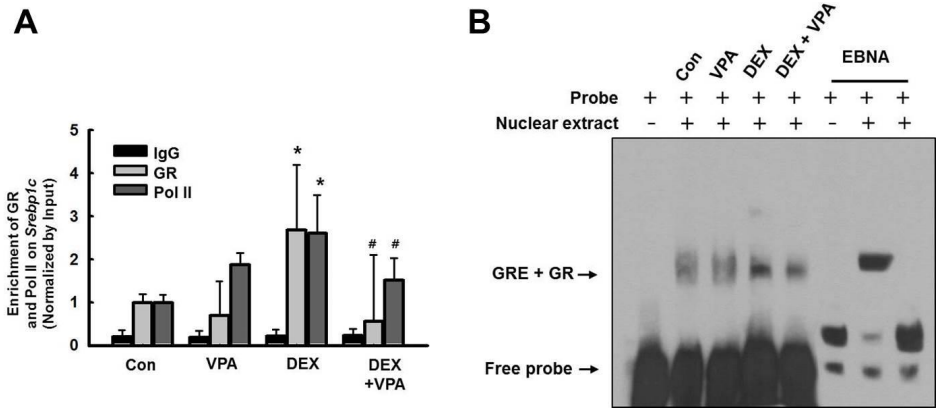

Fig. 7. Effect of VPA treatment on binding of GR or Pol II on GRE of Srebp1c promoter. (A) The enrichment of GR and Pol II at the promoters for *Srebp1c* was analyzed by ChIP. The ChIP assays were quantified by qPCR. Treatment with DEX (10 nM) increased the enrichment of GR and Pol II on the *Srebp1c* promoter, which was decreased by pretreatment with VPA. The graphs show the mean±SE of 3 independent experiments. (*p<0.05 *vs.* control; #p<0.05 *vs.* DEX). (B) EMSA. HepG2 cells were pretreated with or without VPA (10 mM) for 6 h then incubated with DEX (10 nM) for 6 h. DEX induced binding of GR to the GRE, which was decreased by pretreatment with VPA. The gel is representative of 3 independent experiments.

plex was blocked by treatment with VPA (10 mM) for 6 h (lane 5). These findings suggested that VPA decreased the recruitment of GR and Pol II to the promoters of lipogenesis genes, as well as the GR DNA binding activity, *in vitro*.

VPA reduced *Fasn* transcriptional activity and increased the acetylation of GR

To evaluate the transcriptional activity of *Fasn* in response to DEX, we performed a luciferase assay. HepG2 cells were transfected with a luciferase vector driven by the *Fasn* promoter. Treatment with DEX increased the transcriptional activity of *Fasn*,

which was significantly decreased by VPA only in cells transfected with wild-type GR (Fig. 6A). We also used 2 GR mutants, in which 2 lysines in the GR acetylation site were substituted with glutamine (QQ) or arginine (RR) (Vigene Biosciences, CA, USA). We found that the DEX-induced transcriptional activity of *Fasn* was not decreased by VPA in cells transfected with the RR-mutant (Fig. 8). We investigated GR acetylation by blotting with an anti–ac-K antibody after immunoprecipitation with an anti-GR antibody (Fig. 9). GR acetylation was analyzed by western blot with anti–ac-K antibody after immunoprecipitation with anti-GR antibody (Figs. 9A and C). The relative protein expression was quantified by optical densitometry (Figs. 9B and D). GR acetylation was significantly increased in HepG2 cells and ACTH-infused rats after treatment with VPA, compared to controls (Figs. 9B and D). These findings indicated that VPA decreased the DEX-induced transcriptional activity of GR by acetylation.

DISCUSSION

In this report, we demonstrated that the inhibition of HDAC attenuates hepatic steatosis through GR acetylation in experimental CS. We showed that HDACi increased GR acetylation in ACTH-infused rats, which decreased the recruitment of GR and Pol II to the promoters of target genes such as *Fasn*, *Acc* and *Srebp1c*. Treatment with HDACi decreased the transcriptional activity of *Fasn* and GR DNA binding activity induced by DEX in HepG2 cells. Therefore, treatment with HDACi reduced the expression of lipogenic enzymes, including FAS, ACC, SCD1 and SREBP1c, resulting in attenuated lipogenesis and hepatic steatosis via GR acetylation. These results are summarized in Fig. 10.

GC plays an important role in the regulation of lipid homeostasis, signal through the GR [23]. Prolonged exposure to excess

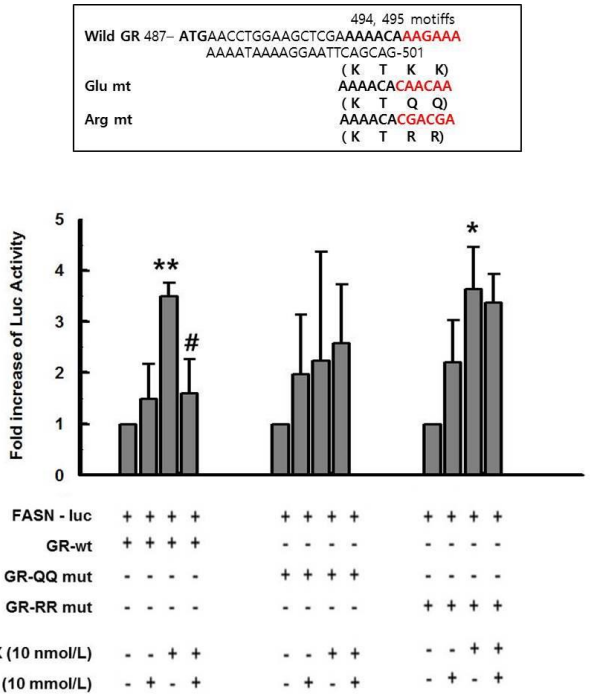

Fig. 8. VPA treatment attenuated *Fasn* transcriptional activity. (A) HepG2 cells were cotransfected with expression vectors for wild-type GR, QQ-mutant GR (Glu mt), or RR-mutant GR (Arg mt), as well as a luciferase vector driven by the *Fasn* promoter. Treatment with DEX increased transcriptional activity in HepG2 cells transfected with wild-type GR and RR-mutant GR, but not the QQ-mutant. Pretreatment with VPA (10 mM) resulted in a significant decrease in DEX-induced promoter activity in HepG2 cells transfected with wild-type GR, but not RR-mutant GR. The graphs show the mean±SE of 5 independent experiments. *p<0.05, **p<0.01 *vs.* control; #p<0.05 *vs.* DEX.

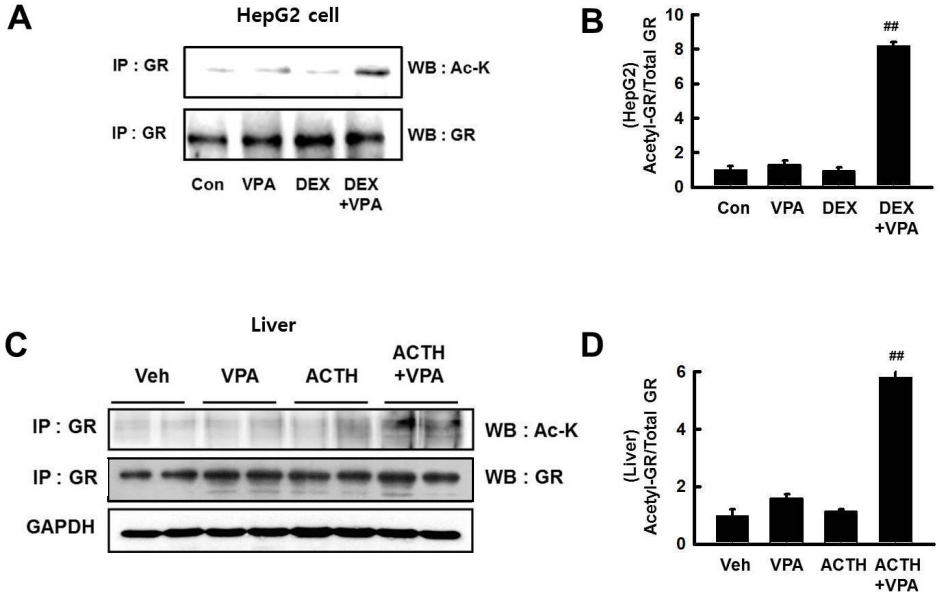

Fig. 9. VPA treatment increased acetylation of GR. (A) HepG2 cells were pretreated with VPA (10 mM) for 3 h then incubated with DEX (10 nM) for 6 h. (C) GR acetylation in rat livers. GR acetylation was analyzed by western blot (WB) with anti–ac-K antibody after immunoprecipitation (IP) with anti-GR antibody. (B and D) The relative protein expression was quantified by optical densitometry (ImageJ software; http://rsbweb.nih.gov). The graphs show the mean±SE of 6 independent experiments. GR acetylation was increased by VPA treatment. ##p<0.01 *vs.* DEX and ACTH.

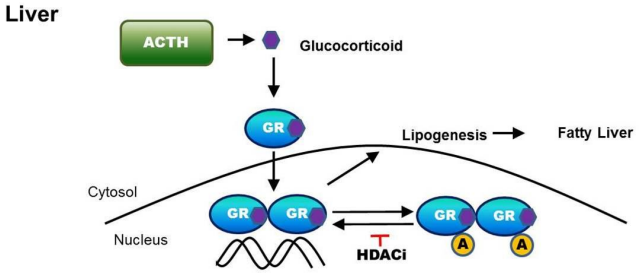

Fig. 10. Summary. HDAC inhibition attenuates hepatic steatosis through GR acetylation in experimental CS.

GCs increases circulating free fatty acid levels and induces ectopic lipid accumulation, which leads to CS [24,25]. We found that the steatosis caused by ACTH infusion was attenuated by the pan-HDACi VPA (Fig. 1). Several studies have reported that HDAC inhibition attenuates adipogenesis and lipid accumulation [26,27].

Acc, *Fasn*, and *Scd1* play important roles in the development of steatosis [28]. De novo lipogenesis involves 2 key enzymes, FAS and ACC; the latter carboxylates acetyl-CoA to form malonyl-CoA, which is further converted by FAS to long-chain fatty acids [29]. SCD1 is the rate-limiting enzyme in the cellular synthesis of monounsaturated fatty acids from saturated fatty acids [30]. We showed that VPA not only attenuates hepatic steatosis, but also reduces expression of lipogenic genes such as *Fasn*, *Acc*, *Scd1*, and *Srebp1c* in ACTH-infused rats (Figs. 1 and 2). In HepG2 cells, pan-HDACi (VPA, SAHA, and TSA) and an HDAC class I-specific inhibitor (MS275) attenuated lipid accumulation and the expression of lipogenesis genes (Fig. 6).

The activity of some steroid hormone receptors is known to be regulated by acetylation. Acetylation of proteins is controlled by HDAC and histone acetyltransferase (HAT), which work in opposition to maintain a balance in physiological conditions [31]. Lysine acetylation at the KTKK motif in the hinge region of the GR by a complex containing 2 proteins, the circadian locomotor output cycles kaput (CLOCK) and brain and muscle aryl hydrocarbon receptor nuclear translocator (ARNT)-like protein 1 (BMAL1), results in the repression of the transcriptional activity of the GR [32]. Acetylation of GR at the KTKK motif attenuates its repressive activity on NF-κB [33]. HDACs play an important role in remodeling chromatin structures [34]. We found that GR acetylation was decreased in ACTH-infused rats and DEX-treated HepG2 cells upon VPA treatment (Fig. 9). The HDACi vorinostat reduces ACTH secretion in CS, though its mechanism has not yet been elucidated [35]. DEX increases transcriptional activity of *Fasn*, which is decreased by VPA (Fig. 8). To confirm that the acetylation of GR by VPA is necessary to attenuate DEX-induced steatosis, we designed two types of GR mutants for luciferase assay (Fig. 8 upper). Our work is the first to report that HDAC inhibition attenuates steatosis through GR acetylation in the context of excess GCs.

The metabolic effects of GCs are mediated by intracellular GR, which associates with genomic GREs to regulate the transcription of GR primary target genes such as *Fasn*, *Acc*, and *Scd1* [9]. The regulation of *Acc* and *Fasn* by GCs has been reported in many organs, including the liver [36,37]. Treatment with VPA decreases the recruitment of GR and Pol II to the promoters of *Fasn*, *Acc*, and *Srebp1c in vivo* (Fig. 3) and *in vitro* (Fig. 7A). Most GR binding regions (GBRs) identified from ChIP sequences are distant from the transcription start site (TSS), whereas less than 10% of GBRs are located within 5 kb upstream of the TSS [38-40]. Although 2 GRE sequences (–71/–65 and –52/–47) were found upstream of the TSS in the rat *Scd1* promoter (Fig. 3C, upper), no significant changes in GR binding to the *Scd1* gene promoters were detected. This may explain why treatment with ACTH had no effect on the recruitment of GR and Pol II to the *Scd1* promoter, despite the presence of the GREs. Though GBRs are being identified in GC-regulated, GR target genes, additional studies are required to verify the role of the GBRs in conferring GC responsiveness. These results suggest that HDAC increases the transcriptional activity of GR by deacetylation, whereas HDACi prevent GR activity by acetylation, in ACTH-infused rats and DEX-treated HepG2 cells.

A recent study report that VPA induced hepatic steatosis and modulated genes associated with lipid metabolism [41]. It is possible that VPA induces low intensity of steatosis. In our study, glucocorticoid obviously contributed to hepatic steatosis, which VPA abrogated. Another study reported that anti-diabetic role of VPA in type-2 diabetes mellitus is mediated by the modulation of insulin signaling and forkhead box protein O1 (FOXO1)-mediated gluconeogenesis [16]. When liver is injured by other effect, VPA is very effective at preventing development of steatosis. The ability of VPA to inhibit glucocorticoid-induced steatosis stands out as being more apparent than its ability to induce steatosis.

In summary, this study presents a mechanism by which HDACi attenuates lipogenesis and hepatic steatosis through GR acetylation in experimental CS. The acetylation of GR decreases the recruitment of GR and Pol II, the DNA binding activity of GR, and the expression of GR target genes that regulate lipogenesis and hepatic steatosis. Therefore, HDACs may be a potential therapeutic target for the treatment of lipogenesis and hepatic steatosis.

ACKNOWLEDGEMENTS

This research was supported by Basic Science Research Program through the National Research Foundation of Korea (NRF) (2015R1D1A1A01056668, 2017R1D1A1B03035335), funded by the Ministry of Education, Science and Technology, and the Korean Health Technology R&D Project, Ministry of Health & Welfare, Republic of Korea (HI13C1527).

CONFLICTS OF INTEREST

The authors declare no conflicts of interest.

SUPPLEMENTARY MATERIALS

Supplementary data including two tables can be found with this article online at http://pdf.medrang.co.kr/paper/pdf/Kjpp/Kjpp022-01-03-s001.pdf.

REFERENCES

1. Lonser RR, Nieman L, Oldfield EH. Cushing's disease: pathobiology, diagnosis, and management. *J Neurosurg.* 2017;126:404-417.
2. Woods CP, Hazlehurst JM, Tomlinson JW. Glucocorticoids and non-alcoholic fatty liver disease. *J Steroid Biochem Mol Biol.* 2015;154:94-103.
3. Chrousos GP. The hypothalamic-pituitary-adrenal axis and immune-mediated inflammation. *N Engl J Med.* 1995;332:1351-1362.
4. Rosen J, Miner JN. The search for safer glucocorticoid receptor ligands. *Endocr Rev.* 2005;26:452-464.
5. Rockall AG, Sohaib SA, Evans D, Kaltsas G, Isidori AM, Monson JP, Besser GM, Grossman AB, Reznek RH. Hepatic steatosis in Cushing's syndrome: a radiological assessment using computed tomography. *Eur J Endocrinol.* 2003;149:543-548.
6. Lazo M, Clark JM. The epidemiology of nonalcoholic fatty liver disease: a global perspective. *Semin Liver Dis.* 2008;28:339-350.
7. Lewis JR, Mohanty SR. Nonalcoholic fatty liver disease: a review and update. *Dig Dis Sci.* 2010;55:560-578.
8. Kassel O, Herrlich P. Crosstalk between the glucocorticoid receptor and other transcription factors: molecular aspects. *Mol Cell Endocrinol.* 2007;275:13-29.
9. Wang JC, Gray NE, Kuo T, Harris CA. Regulation of triglyceride metabolism by glucocorticoid receptor. *Cell Biosci.* 2012;2:19.
10. Lemke U, Krones-Herzig A, Berriel Diaz M, Narvekar P, Ziegler A, Vegiopoulos A, Cato AC, Bohl S, Klingmüller U, Screaton RA, Müller-Decker K, Kersten S, Herzig S. The glucocorticoid receptor controls hepatic dyslipidemia through Hes1. *Cell Metab.* 2008;8:212-223.
11. Mueller KM, Kornfeld JW, Friedbichler K, Blaas L, Egger G, Esterbauer H, Hasselblatt P, Schlederer M, Haindl S, Wagner KU, Engblom D, Haemmerle G, Kratky D, Sexl V, Kenner L, Kozlov AV, Terracciano L, Zechner R, Schuetz G, Casanova E, Pospisilik JA, Heim MH, Moriggl R. Impairment of hepatic growth hormone and glucocorticoid receptor signaling causes steatosis and hepatocellular carcinoma in mice. *Hepatology.* 2011;54:1398-1409.
12. Faus H, Haendler B. Post-translational modifications of steroid receptors. *Biomed Pharmacother.* 2006;60:520-528.
13. Galliher-Beckley AJ, Williams JG, Cidlowski JA. Ligand-independent phosphorylation of the glucocorticoid receptor integrates cellular stress pathways with nuclear receptor signaling. *Mol Cell Biol.* 2011;31:4663-4675.
14. Chrousos GP, Kino T. Intracellular glucocorticoid signaling: a formerly simple system turns stochastic. *Sci STKE.* 2005;2005:pe48.
15. Patel BM, Raghunathan S, Porwal U. Cardioprotective effects of magnesium valproate in type 2 diabetes mellitus. *Eur J Pharmacol.* 2014;728:128-134.
16. Khan S, Kumar S, Jena G. Valproic acid reduces insulin-resistance, fat deposition and FOXO1-mediated gluconeogenesis in type-2 diabetic rat. *Biochimie.* 2016;125:42-52.
17. Buchwald M, Krämer OH, Heinzel T. HDACi–targets beyond chromatin. *Cancer Lett.* 2009;280:160-167.
18. Kadiyala V, Patrick NM, Mathieu W, Jaime-Frias R, Pookhao N, An L, Smith CL. Class I lysine deacetylases facilitate glucocorticoid-induced transcription. *J Biol Chem.* 2013;288:28900-28912.
19. Lauffer BE, Mintzer R, Fong R, Mukund S, Tam C, Zilberleyb I, Flicke B, Ritscher A, Fedorowicz G, Vallero R, Ortwine DF, Gunzner J, Modrusan Z, Neumann L, Koth CM, Lupardus PJ, Kaminker JS, Heise CE, Steiner P. Histone deacetylase (HDAC) inhibitor kinetic rate constants correlate with cellular histone acetylation but not transcription and cell viability. *J Biol Chem.* 2013;288:26926-26943.
20. Kang SH, Seok YM, Song MJ, Lee HA, Kurz T, Kim I. Histone deacetylase inhibition attenuates cardiac hypertrophy and fibrosis through acetylation of mineralocorticoid receptor in spontaneously hypertensive rats. *Mol Pharmacol.* 2015;87:782-791.
21. Lee HA, Lee DY, Cho HM, Kim SY, Iwasaki Y, Kim IK. Histone deacetylase inhibition attenuates transcriptional activity of mineralocorticoid receptor through its acetylation and prevents development of hypertension. *Circ Res.* 2013;112:1004-1012.
22. Lee HA, Song MJ, Seok YM, Kang SH, Kim SY, Kim I. Histone deacetylase 3 and 4 complex stimulates the transcriptional activity of the mineralocorticoid receptor. *PLoS One.* 2015;10:e0136801.
23. Kadmiel M, Cidlowski JA. Glucocorticoid receptor signaling in health and disease. *Trends Pharmacol Sci.* 2013;34:518-530.
24. Macfarlane DP, Forbes S, Walker BR. Glucocorticoids and fatty acid metabolism in humans: fuelling fat redistribution in the metabolic syndrome. *J Endocrinol.* 2008;197:189-204.
25. Arnaldi G, Scandali VM, Trementino L, Cardinaletti M, Appolloni G, Boscaro M. Pathophysiology of dyslipidemia in Cushing's syndrome. *Neuroendocrinology.* 2010;92 Suppl 1:86-90.
26. Lagace DC, Nachtigal MW. Inhibition of histone deacetylase activity by valproic acid blocks adipogenesis. *J Biol Chem.* 2004;279:18851-18860.
27. Catalioto RM, Maggi CA, Giuliani S. Chemically distinct HDAC inhibitors prevent adipose conversion of subcutaneous human white preadipocytes at an early stage of the differentiation program. *Exp Cell Res.* 2009;315:3267-3280.
28. Wakil SJ, Abu-Elheiga LA. Fatty acid metabolism: target for metabolic syndrome. *J Lipid Res.* 2009;50 Suppl:S138-143.
29. Mashima T, Seimiya H, Tsuruo T. De novo fatty-acid synthesis and related pathways as molecular targets for cancer therapy. *Br J Cancer.* 2009;100:1369-1372.
30. Strable MS, Ntambi JM. Genetic control of de novo lipogenesis: role in diet-induced obesity. *Crit Rev Biochem Mol Biol.* 2010;45:199-214.
31. Peserico A, Simone C. Physical and functional HAT/HDAC interplay regulates protein acetylation balance. *J Biomed Biotechnol.* 2011;2011:371832.
32. Nader N, Chrousos GP, Kino T. Circadian rhythm transcription factor CLOCK regulates the transcriptional activity of the glucocor-

ticoid receptor by acetylating its hinge region lysine cluster: potential physiological implications. *FASEB J.* 2009;23:1572-1583.
33. Ito K, Yamamura S, Essilfie-Quaye S, Cosio B, Ito M, Barnes PJ, Adcock IM. Histone deacetylase 2-mediated deacetylation of the glucocorticoid receptor enables NF-κB suppression. *J Exp Med.* 2006;203:7-13.
34. Delcuve GP, Khan DH, Davie JR. Roles of histone deacetylases in epigenetic regulation: emerging paradigms from studies with inhibitors. *Clin Epigenetics.* 2012;4:5.
35. Chittiboina P, Lu J, Wang X, Piazza MG, Zhuang Z. Histone deacetylase inhibitor vorinostat is a novel, promising treatment for cushing disease. *Neurosurgery.* 2016;63 Suppl 1:183.
36. Sul HS, Wang D. Nutritional and hormonal regulation of enzymes in fat synthesis: studies of fatty acid synthase and mitochondrial glycerol-3-phosphate acyltransferase gene transcription. *Annu Rev Nutr.* 1998;18:331-351.
37. Zhao LF, Iwasaki Y, Zhe W, Nishiyama M, Taguchi T, Tsugita M, Kambayashi M, Hashimoto K, Terada Y. Hormonal regulation of acetyl-CoA carboxylase isoenzyme gene transcription. *Endocr J.* 2010;57:317-324.
38. Reddy TE, Pauli F, Sprouse RO, Neff NF, Newberry KM, Garabedian MJ, Myers RM. Genomic determination of the glucocorticoid response reveals unexpected mechanisms of gene regulation. *Genome Res.* 2009;19:2163-2171.
39. So AY, Chaivorapol C, Bolton EC, Li H, Yamamoto KR. Determinants of cell- and gene-specific transcriptional regulation by the glucocorticoid receptor. *PLoS Genet.* 2007;3:e94.
40. Yu CY, Mayba O, Lee JV, Tran J, Harris C, Speed TP, Wang JC. Genome-wide analysis of glucocorticoid receptor binding regions in adipocytes reveal gene network involved in triglyceride homeostasis. *PLoS One.* 2010;5:e15188.
41. Bai X, Hong W, Cai P, Chen Y, Xu C, Cao D, Yu W, Zhao Z, Huang M, Jin J. Valproate induced hepatic steatosis by enhanced fatty acid uptake and triglyceride synthesis. *Toxicol Appl Pharmacol.* 2017;324:12-25.